Virus Research 271 (2019) 197671

Contents lists available at ScienceDirect

Virus Research

journal homepage: www.elsevier.com/locate/virusres

miR-146a promotes Borna disease virus 1 replication through IRAK1/TRAF6/NF-κB signaling pathway

Xiong Zhang[a,b,1], Yujie Guo[b,1], Xiaoyan Xu[b], Tian Tang[b], Lin Sun[b,c], Haiyang Wang[b], Wei Zhou[b], Liang Fang[d], Qi Li[a], Peng Xie[a,b,d,*]

[a] Department of Neurology, The First Affiliated Hospital, Chongqing Medical University, Chongqing, China
[b] Chongqing Key Laboratory of Neurobiology, Chongqing Medical University, Chongqing, China
[c] Department of Pain, The First Affiliated Hospital of Chongqing Medical University, Chongqing, China
[d] Department of Neurology, Yongchuan Hospital, Chongqing Medical University, Chongqing, China

ARTICLE INFO

Keywords:
BoDV-1
HMC3
IRAK1/TRAF6/NF-κB signaling pathway
Immune
miR-146a
Viral replication

ABSTRACT

Background/Aims: : Borna disease virus 1 (BoDV-1) is a negative single-stranded RNA virus that is highly neurotropic. BoDV-1 infection can damage the central nervous system and cause inflammation. To survive in host cells, BoDV-1 must evade the host innate immune response. A previous study showed that miR-146a expression increased in neonatal rats infected with BoDV-1. miR-146a is a microRNA suggested to negatively regulate innate immune and inflammatory responses and antiviral pathways. Many groups have reported that its overexpression facilitates viral replication. However, it is unclear whether miR-146a is involved in escape from the host immune response during BoDV-1 infection.

Methods: : In this study, BoDV-1 was used to infect neonatal rats within 24 h of birth intracranially, as well as to infect human microglial cells (HMC3). miR-146a expression was analyzed by RT-qPCR. The TargetScanHuman database was used to find the target genes of miR-146a. A search of the binding sites of miR-146a and its target gene's 3′-untranslated region (3′UTR) was also performed using RNAhybrid software. The binding sites of miR-146a and the target gene's 3′UTR were detected by dual luciferase reporter assays. Overexpression and suppression studies of miR-146a were performed to determine its effect on BoDV-1 replication. The relative protein expression of members of the IRAK1/TRAF6/NF-κB signaling pathway was also evaluated by western blotting in HMC3.

Results: : After BoDV-1 infection of neurons in vivo and of HMC3 cells, miR-146a expression was significantly upregulated. miR-146a overexpression in HMC3 cells promoted viral replication, while its inhibition inhibited it. Through the TargetScanHuman database, we identified the target genes of anti-inflammatory miR-146a: IRAK1 and TRAF6. We also found that BoDV-1 could inhibit IRAK1 and TRAF6 expression in HMC3 cells. Moreover, we showed that the inhibition of IRAK1 and TRAF6 also led to decreases in the expression of P65 and phosphorylated P65 in the downstream NF-κB pathway. Subsequently, we confirmed the interaction of miR-146a with IRAK1 and TRAF6 by luciferase assay.

Conclusion: : Our results suggest that miR-146a inhibits the IRAK1/TRAF6/NF-κB signaling pathway to facilitate BoDV-1 survival in host cells.

1. Introduction

Borna disease virus 1 (BoDV-1) belongs to the order Mononegavirales, family Bornaviridae, species *Mammalian 1 orthobornavirus*; it is a nonsegmented, negative single-stranded, noncytolytic RNA virus (Bonnaud et al., 2015; Kuhn et al., 2015; Maes et al., 2019; Tizard et al., 2016). BoDV-1 is a highly neurotropic prototype of Bornaviruses and persistently infects the central nervous system of a wide range of vertebrate species (Jie et al., 2018; Vahlenkamp et al., 2002). BoDV-1 infection induces a wide spectrum of neurological diseases, ranging from immune-mediated acute fatal encephalitis to non-inflammatory behavioral changes (Bonnaud et al., 2015; Korn et al., 2018). Recently, BoDV-1 was identified as the cause of deadly human encephalitis after organ transplantation, which markedly increased the

* Corresponding author at: The First Affiliated Hospital of Chongqing Medical University, 1 Youyi Road, Yuzhong District, 400016, Chongqing, China.
E-mail address: xiepeng@cqmu.edu.cn (P. Xie).
[1] These authors contributed equally to this work.

https://doi.org/10.1016/j.virusres.2019.197671
Received 13 March 2019; Received in revised form 19 June 2019; Accepted 17 July 2019
Available online 19 July 2019
0168-1702/

significance of this infection in terms of human health and disease (Korn et al., 2018). It is a major challenge for BoDV-1 to maintain long-term persistent infection in the host cell. The neurological properties of BoDV-1 provide an opportunity to decipher the molecular mechanisms of viral–cell interactions during persistent infection; however, it remains unclear how BoDV-1 escapes the antiviral immune response of its host.

Small noncoding RNAs, termed microRNAs (miRNAs), consist of ˜22 nucleotides and control gene expression by silencing targeted messenger RNAs (mRNAs) translated by specific genes (Finnerty et al., 2010; Fuessel et al., 2018). miRNAs play an important role in numerous processes such as stem cell development and differentiated cell survival, tumorigenesis, cognitive disability, neuronal development and virus replication. miRNAs regulate gene expression via the binding of their seed region to a complementary site in the target gene 3′ UTR. RNA virus infection can modulate cellular miRNA expression, which causes downstream changes in the host transcriptome that can be beneficial to the virus. Additionally, host miRNAs may help the virus to evade antiviral immune responses and enhance its replication (Ambros, 2004; Jiang et al., 2018; Peng and Croce, 2016; Rahman et al., 2019; Sempere et al., 2004; Skalsky and Cullen, 2010; Trobaugh and Klimstra, 2017). miR-122 (Qian et al., 2010) and miR-155 (Zhai et al., 2013) expression is modulated in Borna disease virus infection. miR-146a is also well known to exert anti-inflammatory effects. Previous studies demonstrated that BoDV-1 increased miR-146a expression in the hippocampus of neonatal rats (Zhao et al., 2015). Moreover, viruses such as JEV and DENV have been reported to overexpress miR-146a, which helps them to depress inflammatory cell responses (Sharma et al., 2015; Wu et al., 2013). MicroRNAs target TNF receptor-associated factor 6 (TRAF6) and IL-1 receptor-associated kinase-1 (IRAK1) genes, which encode various adaptor proteins involved in NF-κB activation (Gao et al., 2015; Jiang et al., 2014; Kamali et al., 2016; Mortazavi-Jahromi et al., 2017; Park et al., 2015). Here, through in vivo and vitro studies, we attempted to elucidate the mechanism of action of miR-146a in BoDV-1 replication.

2. Materials and methods

2.1. Animals and ethics statement

Pregnant Sprague–Dawley (SD) rats (n = 2) at 16–18 days of gestation were provided by the animal center of Chongqing Medical University (Chongqing, China) and kept in individual cages prior to the newborn rats being separated from their mothers. BoDV-1 was extracted from an oligodendroglia cell line via freezing and thawing cycles in sterile PBS buffer. Each neonatal rat within 24 h of birth received an injection of 2 µl (1×10^7 FFU/mL) of BoDV-1 inoculum (BoDV-1 strain was a gift from Professor Hanns Ludwig, Free University of Berlin, Germany) or an equal volume of PBS (HyClone, USA) into the left lateral ventricle using a 5-µL Hamilton syringe, as previously described(Zhao et al., 2015). The experimental procedures followed the National Institutes of Health Guide for the Care and Use of Laboratory Animals. All animal experiments were approved by the Research Ethics Committee of Chongqing Medical University.

2.2. Cell culture and viral infection

The human microglial cell line HMC3 was purchased from Shanghai Zhong Qiao Xin Zhou Biotechnology Co. (#ZQ0887; Shanghai, China). HMC3 cells were grown in Complete Eagle's minimum essential medium (MEM) (#ZQ-320; Shanghai Zhong Qiao Xin Zhou Biotechnology Co.) with 10% fetal bovine serum (#A31608-01; Gibco), 100 U penicillin and 100 µg/ml streptomycin (#15140122; Gibco). For infection experiments, 1×10^5 HMC3 cells were seeded in six-well dishes and infected with BoDV-1 at MOI 5 in complete MEM for 48 h.

Table 1
Sequences of RNA oligos used.

Name of oligos	Sequences
hsa-miR-146a-5p mimics	5′-UGAGAACUGAAUUCCAUGGGUU-3′
microRNA mimics N.C	5′-UUGUACUACACAAAAGUACUG-3′
hsa-miR-146a-5p inhibitor	5′-AACCCAUGGAAUUCAGUUCUCA-3′
microRNA inhibitor N.C	5′-CAGUACUUUUGUGUAGUACAA-3′

2.3. miR-146a transfection

HMC3 cells were seeded in six-well dishes, and 200 pmol miR-146a-5p mimic, inhibitor, or miRNA N.C. (Shanghai GenePharma Co., Shanghai, China) was transfected using TransIntroTM EL Transfection Reagent (Transgen Biotech, China), in accordance with the manufacturer's protocol. The sequences of miR-146a mimic, inhibitor and miRNA N.C. are presented in Table 1. The cells were harvested at 48 h post-transfection for RNA isolation and Western blotting.

2.4. RNA isolation and real-time quantitative polymerase chain reaction (RT-qPCR)

Total RNA was extracted with TRIzol, after which reverse transcription with 5 × PrimeScript RT Master Mix (TaKaRa, Japan) was performed, in accordance with the manufacturer's protocols. RT-qPCR was carried out using 2 × T5 Fast qPCR Mix (SYBR Green I) (Tsingke Biologic Technology, China) with a LightCycler® 96 Real-Time qPCR Detection system (Roche, Switzerland). Thermocycling conditions consisted of an initial denaturation step for 300 s at 95 °C, followed by 40 cycles of 95 °C for 30 s and 55 °C for 45 s. The relative quantities of amplified product were calculated using the comparative cycle threshold (Ct) method. Data were derived from three independent amplifications. The primer sequences used for real-time PCR are listed in Table 2. GAPDH or Actin was used as a reference gene.

miR-146a was synthesized from total RNA using stem-loop reverse transcription primer with a PrimeScript™ RT Reagent Kit with gDNA Eraser (TaKaRa), in accordance with the manufacturer's protocols, and then quantified by real-time qPCR. Fold variations between RNA samples were calculated after normalization to U6. The sequences of the primers and probes used in the current study are shown in Table 2.

Table 2
Sequences of primers used in this study.

Gene and oligonucleotide	Sequences
BDV P40	
PCR forward primer	5′-GGTTTAAAACTATGATGGCAGCCTTA-3′
PCR reverse primer	5′-GTGGATTAAACATCTGGAGTAGTGTAGC-3′
BDV P24	
PCR forward primer	5′-TCCCTGGAGGACGAAGAAGAT-3′
PCR reverse primer	5′-CTTCCGTGGTCTTGGTGACC-3′
ACTIN	
PCR forward primer	5′-CAGCCATGTACGTTGCTATCCAGG-3′
PCR reverse primer	5′-AGGTCCAGACGCAGGATGGCATG-3′
GAPDH	
PCR forward primer	5′-TGACTCTACCCACGGCAAG -3′
PCR reverse primer	5′-TACTCAGCACCAGCATCACC -3′
miR-146a-5p	
RT primer	5′-GTCGTATCCAGTGCGTGTCGTGGAGTC GGCAATTGCACTGGATACGACAACCCA-3′
PCR forward primer	5′-GGGTGAGAACTGAATTCCA-3′
PCR reverse primer	5′-CAGTGCGTGTCGTGGAGT-3′
U6	
RT primer	5′-AACGCTTCACGAATTTGCGT-3′
PCR forward primer	5′-CTCGCTTCGGCAGCACA-3′
PCR reverse primer	5′-AACGCTTCACGAATTTGCGT-3′

2.5. Western blotting

The harvested cell pellet was lysed using a protease inhibitor cocktail (KeyGEN Biotech Co., China). Protein concentration was determined using the bicinchoninic acid assay (BCA), separated using 4%–20% ExpressPlus™ PAGE Gel and transferred to polyvinylidene difluoride membranes (EMD Millipore, USA). The membranes were blocked with 5% nonfat dried milk in TBST for 4 h and then incubated with the following antibodies overnight at 4 °C: anti-IRAK1 (Cell Signaling Technology, Danvers, USA; 1:1000), TRAF6 (Cell Signaling Technology; 1:1000), anti-phospho-NF-κB p65 (Cell Signaling Technology; 1:1000), anti-NF-κB p65 (Cell Signaling Technology; 1:1000), P40 antibodies (Abgent, Inc., Santa Diego, CA, USA; 1:500), β-tubulin antibodies (Cell Signaling Technology; 1:1000) and GAPDH antibodies (Hangzhou Goodhere Biotechnology Co., China). Next, three washes with TBST for 10 min each were performed. Later, the membrane was incubated in horseradish peroxidase-conjugated secondary antibodies for 2 h and then washed three times with TBST (for 15 min each). Blots were visualized using an enhanced chemiluminescence kit (EMD Millipore). Each sample was quantified using Quantity One software (Bio-Rad Laboratories Inc., USA). All experiments were performed in triplicate under the same conditions.

2.6. Plasmid construction

Target genes of hsa-miR-146a-5p were predicted using the TargetScan database. Subsequently, the desired genes were detected, namely, IRAK1 and TRAF6. Binding sites of their 3′UTRs and hsa-miR-146a-5p were identified using the RNAhybrid database. Segmented 3′UTRs of the IRAK1 and TRAF6 genes were amplified. After sequencing validation, these fragments were inserted into the Psicheck-2 Vector to construct recombinant plasmids containing two different haplotypes: Psicheck-2-IRAK1-3′-UTR-WT and Psicheck-2-TRAF6-3′-UTR -WT. The sequences of the segmented 3′UTRs used are shown in Table 3.

2.7. Transfection and dual luciferase reporter assays

HMC3 cells were seeded in 12-well dishes and transfected with IRAK1 and TRAF6 luciferase reporter plasmids (100 ng) using TransIntro™ EL Transfection Reagent (5 μl). For miR-146a overexpression experiments, 200 pmol miRNA N.C. mimic and hsa-miR-146a-5p mimic were cotransfected along with plasmids and luciferase activity was measured 48 h later. To measure the luminescence activity, cells were lysed in 1 × lysis buffer provided with the Dual-Luciferase® Reporter Assay System (Promega, China) and luminescence was measured by adding luciferase assay reagent as per the manufacturer's protocol. Luciferase activity was measured using a GloMax 20/20 Luminometer (Promega).

Table 3
Sequences of segmented 3′UTRs used.

Name of segmented 3′UTRs	Sequences
IRAK1-3'UTR-WT	5′-Ctcgagtgtgttcacctgggcagatcccccaaatccgga agtcaaagttctcatggtcagaagttctcatggtgcacgagtcctcagc actctgccggcagtgggggtgggggcccatgcccgcgggggagag aaggaggtggccctgctgttctaggctctgtgggcataggcaggcag agtggaaccctgcctccatgccagcatctgggggcaaggaaggctg gcatcatccagtgaggaggctggcgcatgttgggaggctgctggctg cacagacccgtgaggggaggagaggggctgctgtgcaggggtgtg gagtagggagctggctcccctgagagccatgcagggcgtctgcagc ccaggcctctggcagcagctctttgcccatctctttggacaggcggccgc-3′
TRAF6-3'UTR -WT	5′-ctcgagtagaatcctggaagtaaccagattttcctaatagggа gatgatttttttgtgtgccatcatgtatttgttaaaggcctatatatagatat aaaatatcgtggaatctagttctcagggagacccgcaactagtataa gcttataaaggatctaaagatccatccaccatttaaagttgtctggtaat gagagatgacattgtatccccagagaggccaaatcagagtcgcca gccagcgttctagatcagccttaatttcaagagaaagccaaggacct catctgcaggggagtgtggttttcagccccagcgagtgtcactttgaac tttccctttgctttttttctctcttctccctcccacccacccttaggctcctgat ctggtgagtttgttatggaggcggccgc-3′

2.8. Statistical analysis

All experiments were performed in triplicate and comparisons were made between all datasets by one-tailed, unpaired Student's *t*-test or one-way ANOVA. Differences were considered significant when $P < 0.05$. * denotes $P < 0.05$, ** denotes $P < 0.01$, and *** denotes $P < 0.001$.

3. Results

3.1. miR-146a is upregulated during BoDV-1 infection

To investigate miR-146a expression during BoDV-1 infection, BoDV-1-specific antibody p40 was used to identify BoDV-1 in rats 8 weeks post-infection, or in HMC3 48 h post-infection. The infectivity of the cells or tissues is shown in the Supplementary Material (Figure S1 and Figure S2), as revealed by immunofluorescence and western blotting. Our data demonstrated that miR-146a expression in the hippocampus of neonatal rats infected with BoDV-1 was significantly higher than in the control group (Fig. 1A). Moreover, miR-146a expression in the HMC3 cells (Fig. 1B) was significantly increased than in the control group. Taken together, these results indicate that miR-146a was upregulated during BoDV-1 infection.

3.2. miR-146a promotes BoDV-1 replication

To explore whether miR-146a has a relationship with viral replication, we transfected HMC3 cells with miR-146a mimic, inhibitor, or N.C. and after 24 h later performed co-infection with BoDV-1. We found a significant increase of viral RNA levels at 24 h post-infection in the miR-146a mimic group compared with that in the N.C. group (Fig. 2A). When endogenous miR-146a was inhibited by transfection with miR-146a inhibitor, a clear downward trend in the number of viral copies was observed at 24 h post-infection was observed (Fig. 2B). We also examined the effect of miR-146a on viral protein expression; induction of BoDV-1 P40 protein expression in miR-146a-overexpressing HME3 cells was found compared with the level in the control (Fig. 2C, D). Therefore, our results reveal that miR-146a produces a virus-friendly environment in cells and promotes BoDV-1 replication.

3.3. BoDV-1 infection downregulates the expression of TRAF6, IRAK1, P65 and phospho-P65

Owing to the expression of miR-146a induced by BoDV-1 infection, we focused on the downstream application of BoDV-1 in our study. Using the TargetScanHuman7.1 database, we predicted that the miR-146a target genes include IRAK1 and TRAF6. We examined the levels of these miR-146a target genes 24 h after BoDV-1 infection. Their expression was downregulated 24 h after BoDV-1 infection compared with that in the control (Fig. 3A). Because these genes are the main adaptor molecules involved in the activation of NF-κB, we determined the level of phospho-p65, a subunit of NF-κB activator complex and found decreases of phospho-p65 and P65 after BoDV-1 infection (Fig. 3C). These results may suggest that miR-146a suppresses the IRAK1/TRAF6/NF-κB pathway to produce an anti-inflammatory milieu in the host cell, which in turn promotes virus survival.

3.4. miR-146a targets TRAF6 and IRAK1 genes

Using RNAhybrid 2.2 software, we predicted that miR-146a

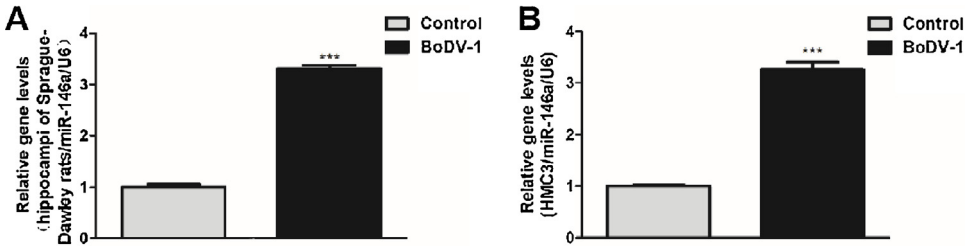

Fig. 1. BoDV-1 infection upregulates miR-146a. (A) The hippocampus of Sprague–Dawley rats was infected with BoDV-1 for 8 weeks. RT-qPCR was used to determine miR-146a levels. (B) The human brain microglial cell line HMC3 was infected with BoDV-1 (MOI = 5) and cells were harvested 48 h later. The $2^{-\Delta\Delta Ct}$ method was used to calculate the expression level of each sample. The C_q value of no template controls (NTCs) > 40. Data represent the mean (± SE) of three independent repeats. ***, $P < 0.001$ (Student's unpaired two-tailed *t*-test).

specifically binds to the 3′UTR of IRAK1 and TRAF6 (Fig. 4A, B), suggesting the interaction between miR-146a and IRAK1/TRAF6 genes. To assess this possible interaction, dual luciferase reporter assays were performed. HMC3 cells were seeded in 12-well dishes and were transfected with IRAK1 and TRAF6 luciferase reporter plasmid using TransIntro™ EL Transfection Reagent. For miR-146a overexpression experiments, 200 pmol microRNA N.C mimics and hsa-miR-146a-5p mimics were co-transfected along with plasmids and luciferase activity was measured 48 h later. There was a significant downward trend of the luciferase activity upon the co-transfection of IRAK1 and miR-146a compared with that in the N.C group. The luciferase activity upon co-transfection with TRAF6 and miR-146a was found to be reduced compared with that upon co-transfection with TRAF6 and N.C.mimics (Fig. 4D).

4. Discussion

In this study, when neonatal Sprague–Dawley rats were infected with BoDV-1 for 8 weeks, the miR-146a level in hippocampus showed a significant increase. Additionally, by overexpressing miR-146a in HMC3, we observed its positive effect on BoDV-1 replication. Moreover, this effect was shown to be related to the IRAK1/TRAF6/NF-κB signaling pathway, in which the relative protein expression of IRAK1, TRAF6 and NF-κB was inhibited when HMC3 cells were infected with BoDV-1, compared with their levels in the control. Additionally, RNAhybrid 2.2 software predicted that miR-146a specifically binds to the 3′UTR of IRAK1 and TRAF6. Taking these findings together, BoDV-1-induced miR-146a upregulation inhibits cellular inflammatory responses to create a cellular milieu that is suitable for viral survival.

Previous evidence suggested that miR-146a promotes viral replication, such as that of Japanese encephalitis virus (JaOArS982 strain), DENV, bronchitis virus, Chikungunya virus, and HBV (Liu et al., 2018; Selvamani et al., 2014; Sharma et al., 2015; Wang and Li, 2018; Wu et al., 2013). In this study, BoDV-1 infection increased miR-146a expression in neurons in vivo and in HMC3 cells. miR-146a overexpression in HMC3 cells promoted viral replication, while its inhibition inhibited it. Recently, a study also demonstrated that miR-146a overexpression facilitated influenza A virus (IAV) replication, while its downregulation suppressed its replication (Zhang et al., 2019). This is generally consistent with our results.

The induction of miR-146a expression was shown to be NF-κB-dependent, as revealed by promoter analysis (Taganov et al., 2006). A

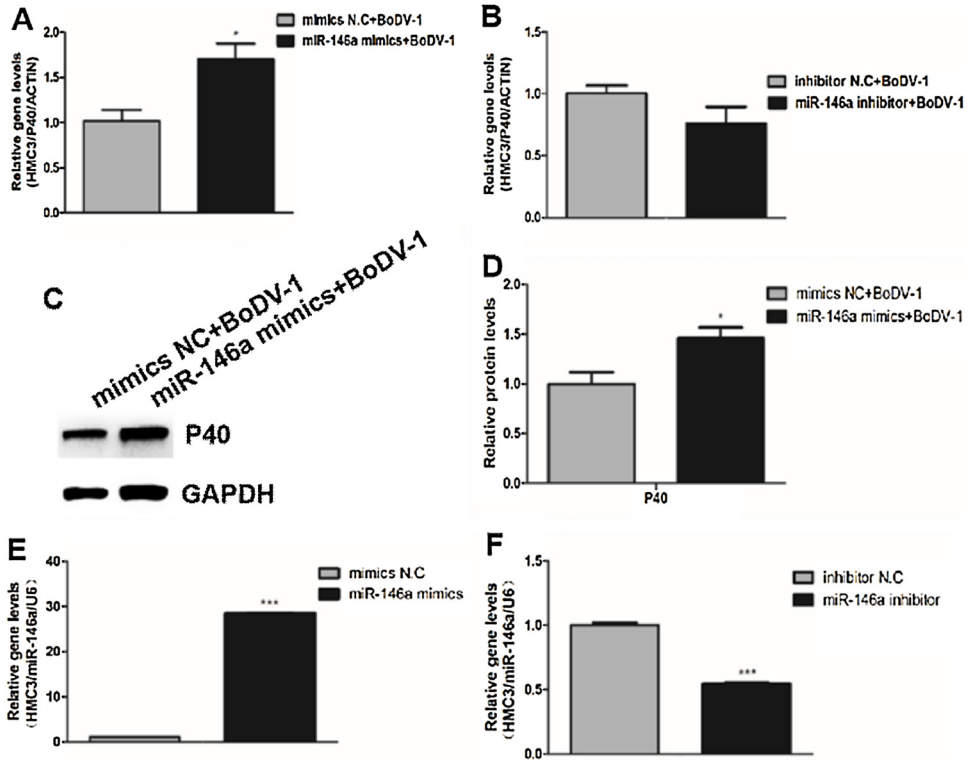

Fig. 2. miR-146a enhances viral replication. (A) HMC3 cells were transfected with miR-146a mimic and microRNA mimics N.C sequence. (B) HMC3 cells were transfected with miR-146a inhibitor and microRNA inhibitor N.C sequence. The cells were infected by BoDV-1 (MOI = 5) and harvested 24 h later. Viral RNA level was determined by RT-qPCR using BoDV-1 P40-specific primers. The $2^{-\Delta\Delta Ct}$ method was used to calculate the expression level of each sample. The C_q value of no template controls (NTCs) > 40. Data represent the mean (± SE) of three independent repeats. *, $P < 0.05$ (Student's unpaired two-tailed *t*-test). (C) Western blots showing the upregulation of viral P40 protein in miR-146a-overexpressing cells. (D) Graph bars represent a densitometry plot depicting the upregulation of P40 protein after miR-146a overexpression. Each sample was quantified using Quantity One software. Data represents the mean (± SE) of three independent repeats. *, $P < 0.05$ (Student's unpaired two-tailed *t*-test). (E) RT-qPCR analysis of miR-146a levels in miR-146a-overexpressing cells for 48 h post-transfection. (F) RT-qPCR analysis of miR-146a levels in miR-146a-suppressed cells. In total, 200 pmol N.C. mimic sequence and miR-146a mimic were used. N.C. mimic group and N.C. inhibitor group were used as controls for comparison. The $2^{-\Delta\Delta Ct}$ method was used to calculate the expression level of each sample. The C_q value of no template controls (NTCs) > 40. Data represent the mean (± SE) of three independent repeats. ***, $P < 0.001$ (Student's unpaired two-tailed *t*-test).

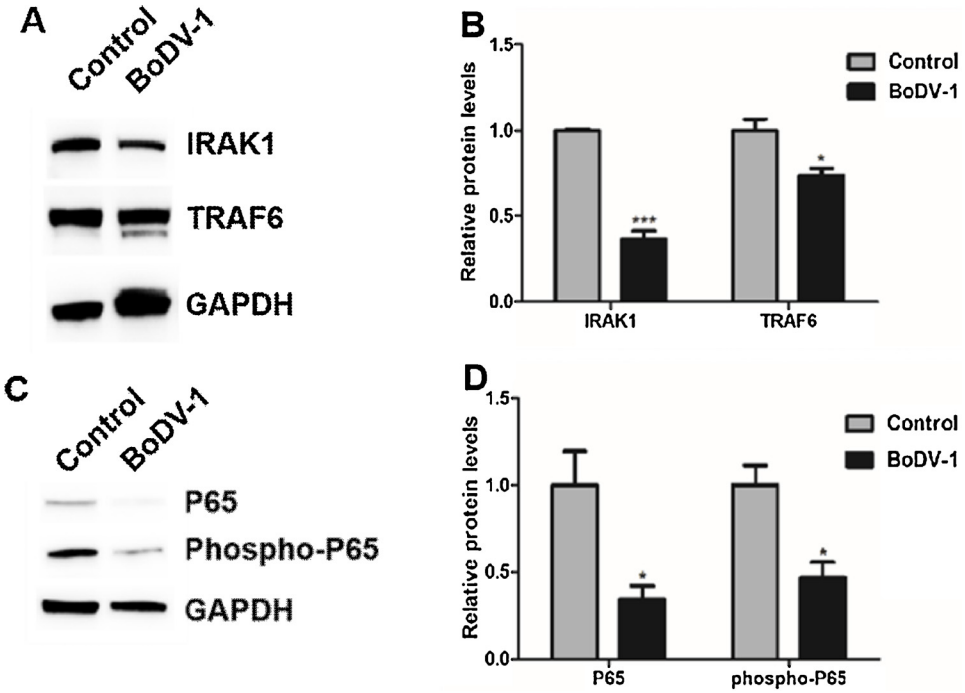

Fig. 3. BoDV-1 downregulates the expression of TRAF6, IRAK1, P65 and phospho-P65. HMC3 cells were infected by BoDV-1 (MOI-5) and harvested 24 h after infection. (A) Western blots showed that the protein expression of TRAF6 and IRAK1 was downregulated after BoDV-1 infection. (B) Graph bars representing a densitometry plot depict the downregulation of TRAF6 and IRAK1 after BoDV-1 infection. (C) Western blot showing the downregulation of phospho-P65 and P65 upon BoDV-1 infection. (D) Densitometry plot showing decreased P65 and phosphorylated P65. Each sample was quantified using Quantity One software. Data represent the mean (± SE) of three independent repeats. *, $P < 0.05$; ***, $P < 0.001$ (Student's unpaired two-tailed *t*-test).

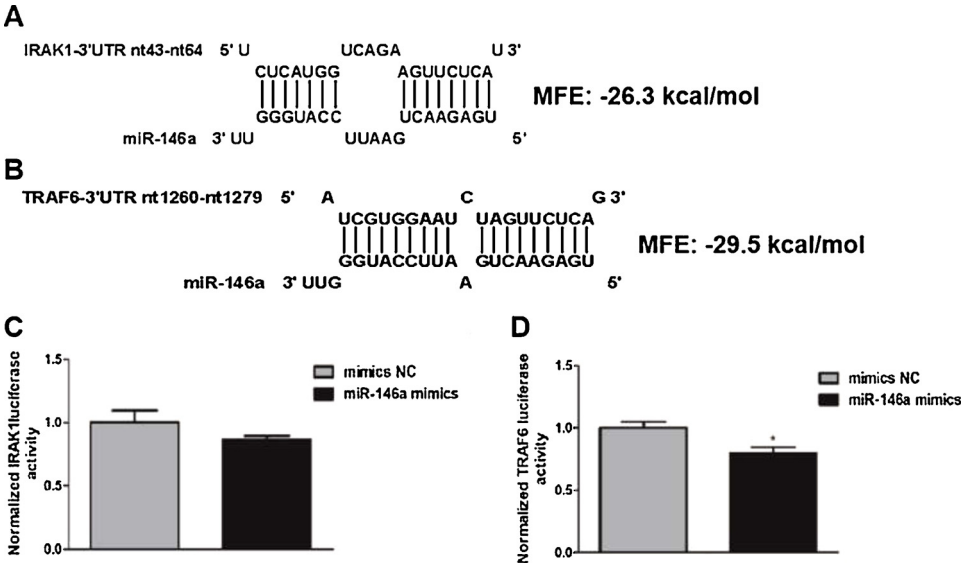

Fig. 4. miR-146a targets TRAF6 and IRAK1 genes. (A, B) Using RNAhybrid 2.2 software, it was predicted that miR-146a specifically bound to the 3′UTR of IRAK1 (A) and TRAF6 (B); the minimum free energy (MFE) between them was also predicted. Detection of luciferase activity of IRAK1 and TRAF6 after cotransfection of IRAK1 and TRAF6 fluorescein reporter plasmids with miR-146a mimics and N.C. mimics 48 h post-transfection in HMC3 cells. (C) Graph bar shows the downward trend of IRAK1 luciferase activity at 48 h after cotransfection. (D) Densitometry plot showing decreased TRAF6 luciferase activity at 48 h after cotransfection. One-way ANOVA was used to determine the statistical significance of differences. P values were considered significant at *, $P < 0.05$.

previous study confirmed that miR-146a acted as a negative feedback regulator of the immune response by targeting two genes (adapter proteins), TRAF6 and IRAK1, which are crucial for proinflammatory signaling. It was also reported that miR-146a inhibited the immune response via the suppression of NF-κB activation by targeting TRAF6, IRAK1 and IRAK2 genes and by negatively regulating the production of proinflammatory cytokines in human microglial cells during Japanese encephalitis virus infection (Sharma et al., 2015). Additionally, miR-146 deficiency in Treg cells was shown to cause a defect in their suppressor function and IFNγ-dependent immune-mediated lesions, apparently through the upregulation of signal transducer and activator 1 (Stat1) expression and activation (Lu et al., 2010). Increased NF-κB activity in the presence of BDV results in the induction of antiviral pathways, reducing the viral titer (Bourteele et al., 2005). Using RNAhybrid software, we determined that TRAF6 and IRAK1 harbor potential miR-146a binding sites in their 3′UTR, which suggests that they are target genes of miR-146a. Using dual luciferase reporter assays, we confirmed that IRAK1 and TRAF6 were the target genes of miR-146a. Furthermore, we showed that BDV infection downregulated the expression of IRAK1 and TRAF6 genes and inhibited the expression of p65 and its phosphorylated protein NF-κB in human microglial cells. Hence, BoDV-1 can inhibit the host's immune response by promoting miR-146a expression and inhibiting the IRAK1/TRAF6/NF-κB signaling pathway.

In summary, we have presented a new mechanism behind persistent BDV infection. miR-146a is involved in facilitating BoDV-1 replication and suppressing the IRAK1/TRAF6/NF-κB signaling pathway. These results suggest that host miRNAs target and participate in a regulatory network between sustained viral infection and host immune response, which provides a basis for studying the regulation of miRNAs in the persistent infection of other viruses. BoDV-1 replication decreased after miR-146a expression inhibition, so the regulation of miRNA-146a expression could provide a new strategy for treating persistent BoDV-1 infection.

Acknowledgements

We thank Professor Hanns Ludwig, Berlin Free University, Germany, and Dr. Liv Bode, Robert Koch Institute, Germany, for providing BoDV-1 strain Hu-H1. This work was supported by the National Key Research and Development Program of China (Grant No. YFA0505700) and the Natural Science Foundation of China (Grant No.81601207). We also thank Liwen Bianji, Edanz Group China (www.liwenbianji.cn/ac), for editing the English text of a draft of this manuscript.

Appendix A. Supplementary data

Supplementary material related to this article can be found, in the online version, at doi:https://doi.org/10.1016/j.virusres.2019.197671.

References

Ambros, V., 2004. The functions of animal microRNAs. Nature 431 (7006), 350–355.
Bonnaud, E.M., Szelechowski, M., Betourne, A., Foret, C., Thouard, A., Gonzalez-Dunia, D., Malnou, C.E., 2015. Borna disease virus phosphoprotein modulates epigenetic signaling in neurons to control viral replication. J. Virol. 89 (11), 5996–6008.
Bourteele, S., Oesterle, K., Pleschka, S., Unterstab, G., Ehrhardt, C., Wolff, T., Ludwig, S., Planz, O., 2005. Constitutive activation of the transcription factor NF-kappaB results in impaired borna disease virus replication. J. Virol. 79 (10), 6043–6051.
Finnerty, J.R., Wang, W.X., Hebert, S.S., Wilfred, B.R., Mao, G., Nelson, P.T., 2010. The miR-15/107 group of microRNA genes: evolutionary biology, cellular functions, and roles in human diseases. J. Mol. Biol. 402 (3), 491–509.
Fuessel, S., Lohse-Fischer, A., Vu Van, D., Salomo, K., Erdmann, K., Wirth, M.P., 2018. Quantification of MicroRNAs in urine-derived specimens. Methods Mol. Biol. 1655, 201–226.
Gao, M., Wang, X., Zhang, X., Ha, T., Ma, H., Liu, L., Kalbfleisch, J.H., Gao, X., Kao, R.L., Williams, D.L., Li, C., 2015. Attenuation of cardiac dysfunction in polymicrobial Sepsis by MicroRNA-146a is mediated via targeting of IRAK1 and TRAF6 expression. J. Immunol. 195 (2), 672–682.
Jiang, J., Song, Z., Zhang, L., 2018. miR-155-5p promotes progression of acute respiratory distress syndrome by inhibiting differentiation of bone marrow mesenchymal stem cells to alveolar type II epithelial cells. Med. Sci. Monit. 24, 4330–4338.
Jiang, W., Kong, L., Ni, Q., Lu, Y., Ding, W., Liu, G., Pu, L., Tang, W., Kong, L., 2014. miR-146a ameliorates liver ischemia/reperfusion injury by suppressing IRAK1 and TRAF6. PLoS One 9 (7), e101530.
Jie, J., Xu, X., Xia, J., Tu, Z., Guo, Y., Li, C., Zhang, X., Wang, H., Song, W., Xie, P., 2018. Memory impairment induced by borna disease virus 1 infection is associated with reduced H3K9 acetylation. Cell. Physiol. Biochem. 49 (1), 381–394.
Kamali, K., Korjan, E.S., Eftekhar, E., Malekzadeh, K., Soufi, F.G., 2016. The role of miR-146a on NF-κB expression level in human umbilical vein endothelial cells under hyperglycemic condition. Bratislava Med. J. 117 (07), 376–380.
Korn, K., Coras, R., Bobinger, T., Herzog, S.M., Lucking, H., Stohr, R., Huttner, H.B., Hartmann, A., Ensser, A., 2018. Fatal encephalitis associated with borna disease virus 1. N. Engl. J. Med. 379 (14), 1375–1377.
Kuhn, J.H., Durrwald, R., Bao, Y., Briese, T., Carbone, K., Clawson, A.N., deRisi, J.L., Garten, W., Jahrling, P.B., Kolodziejek, J., Rubbenstroth, D., Schwemmle, M., Stenglein, M., Tomonaga, K., Weissenbock, H., Nowotny, N., 2015. Taxonomic re-organization of the family Bornaviridae. Arch. Virol. 160 (2), 621–632.
Liu, H., Yang, X., Zhang, Z.-k., Zou, W.-c., Wang, H.-n., 2018. miR-146a-5p promotes replication of infectious bronchitis virus by targeting IRAK2 and TNFRSF18. Microb. Pathog. 120, 32–36.
Lu, L.F., Boldin, M.P., Chaudhry, A., Lin, L.L., Taganov, K.D., Hanada, T., Yoshimura, A., Baltimore, D., Rudensky, A.Y., 2010. Function of miR-146a in controlling Treg cell-mediated regulation of Th1 responses. Cell 142 (6), 914–929.
Maes, P., Amarasinghe, G.K., Ayllon, M.A., Basler, C.F., Bavari, S., Blasdell, K.R., Briese, T., Brown, P.A., Bukreyev, A., Balkema-Buschmann, A., Buchholz, U.J., Chandran, K., Crozier, I., de Swart, R.L., Dietzgen, R.G., Dolnik, O., Domier, L.L., Drexler, J.F., Durrwald, R., Dundon, W.G., Duprex, W.P., Dye, J.M., Easton, A.J., Fooks, A.R., Formenty, P.B.H., Fouchier, R.A.M., Freitas-Astua, J., Ghedin, E., Griffiths, A., Hewson, R., Horie, M., Hurwitz, J.L., Hyndman, T.H., Jiang, D., Kobinger, G.P., Kondo, H., Kurath, G., Kuzmin, I.V., Lamb, R.A., Lee, B., Leroy, E.M., Li, J., Marzano, S.L., Muhlberger, E., Netesov, S.V., Nowotny, N., Palacios, G., Palyi, B., Paweska, J.T., Payne, S.L., Rima, B.K., Rota, P., Rubbenstroth, D., Simmonds, P., Smither, S.J., Song, Q., Song, T., Spann, K., Stenglein, M.D., Stone, D.M., Takada, A., Tesh, R.B., Tomonaga, K., Tordo, N., Towner, J.S., van den Hoogen, B., Vasilakis, N., Wahl, V., Walker, P.J., Wang, D., Wang, L.F., Whitfield, A.E., Williams, J.V., Ye, G., Zerbini, F.M., Zhang, Y.Z., Kuhn, J.H., 2019. Taxonomy of the order Mononegavirales: second update 2018. Arch. Virol.
Mortazavi-Jahromi, S.S., Jamshidi, M.M., Farazmand, A., Aghazadeh, Z., Yousefi, M., Mirshafiey, A., 2017. Pharmacological effects of beta-d-mannuronic acid (M2000) on miR-146a, IRAK1, TRAF6 and NF-kappaB gene expression, as target molecules in inflammatory reactions. Pharmacol. Rep. 69 (3), 479–484.
Park, H., Huang, X., Lu, C., Cairo, M.S., Zhou, X., 2015. MicroRNA-146a and microRNA-146b regulate human dendritic cell apoptosis and cytokine production by targeting TRAF6 and IRAK1 proteins. J. Biol. Chem. 290 (5), 2831–2841.
Peng, Y., Croce, C.M., 2016. The role of MicroRNAs in human cancer. Signal Transduct. Target. Ther. 1, 15004.
Qian, J., Zhai, A., Kao, W., Li, Y., Song, W., Fu, Y., Chen, X., Zhang, Q., Wu, J., Li, H., Zhong, Z., Ling, H., Zhang, F., 2010. Modulation of miR-122 on persistently Borna disease virus infected human oligodendroglial cells. Antiviral Res. 87 (2), 249–256.
Rahman, M.R., Islam, T., Turanli, B., Zaman, T., Faruquee, H.M., Rahman, M.M., Mollah, M.N.H., Nanda, R.K., Arga, K.Y., Gov, E., Moni, M.A., 2019. Network-based approach to identify molecular signatures and therapeutic agents in Alzheimer's disease. Comput. Biol. Chem. 78, 431–439.
Selvamani, S.P., Mishra, R., Singh, S.K., 2014. Chikungunya virus exploits miR-146a to regulate NF-kappaB pathway in human synovial fibroblasts. PLoS One 9 (8), e103624.
Sempere, L.F., Freemantle, S., Pitha-Rowe, I., Moss, E., Dmitrovsky, E., Ambros, V., 2004. Expression profiling of mammalian microRNAs uncovers a subset of brain-expressed microRNAs with possible roles in murine and human neuronal differentiation. Genome Biol. 5 (3), R13.
Sharma, N., Verma, R., Kumawat, K.L., Basu, A., Singh, S.K., 2015. miR-146a suppresses cellular immune response during Japanese encephalitis virus JaOArS982 strain infection in human microglial cells. J. Neuroinflammation 12, 30.
Skalsky, R.L., Cullen, B.R., 2010. Viruses, microRNAs, and host interactions. Annu. Rev. Microbiol. 64, 123–141.
Taganov, K.D., Boldin, M.P., Chang, K.J., Baltimore, D., 2006. NF-kappaB-dependent induction of microRNA miR-146, an inhibitor targeted to signaling proteins of innate immune responses. Proc Natl Acad Sci U S A 103 (33), 12481–12486.
Tizard, I., Ball, J., Stoica, G., Payne, S., 2016. The pathogenesis of bornaviral diseases in mammals. Anim. Health Res. Rev. 17 (2), 92–109.
Trobaugh, D.W., Klimstra, W.B., 2017. MicroRNA regulation of RNA virus replication and pathogenesis. Trends Mol. Med. 23 (1), 80–93.
Vahlenkamp, T.W., Konrath, A., Weber, M., Muller, H., 2002. Persistence of borna disease virus in naturally infected sheep. J. Virol. 76 (19), 9735–9743.
Wang, Y., Li, Y., 2018. miR-146 promotes HBV replication and expression by targeting ZEB2. Biomed. Pharmacother. 99, 576–582.
Wu, S., He, L., Li, Y., Wang, T., Feng, L., Jiang, L., Zhang, P., Huang, X., 2013. miR-146a facilitates replication of dengue virus by dampening interferon induction by targeting TRAF6. J. Infect. 67 (4), 329–341.
Zhai, A., Qian, J., Kao, W., Li, A., Li, Y., He, J., Zhang, Q., Song, W., Fu, Y., Wu, J., Chen, X., Li, H., Zhong, Z., Ling, H., Zhang, F., 2013. Borna disease virus encoded phosphoprotein inhibits host innate immunity by regulating miR-155. Antiviral Res. 98 (1), 66–75.
Zhang, F., Sun, X., Zhu, Y., Qin, W., 2019. Downregulation of miR-146a inhibits influenza A virus replication by enhancing the type I interferon response in vitro and in vivo. Biomed. Pharmacother. 111, 740–750.
Zhao, M., Sun, L., Chen, S., Li, D., Zhang, L., He, P., Liu, X., Zhang, L., Zhang, H., Yang, D., Huang, R., Xie, P., 2015. Borna disease virus infection impacts microRNAs associated with nervous system development, cell differentiation, proliferation and apoptosis in the hippocampi of neonatal rats. Mol. Med. Rep. 12 (3), 3697–3703.